Plant Soil
https://doi.org/10.1007/s11104-026-08947-0

RESEARCH ARTICLE

Soil–plant interactions during early vegetation growth govern HONO, NO and N_2O emissions through moisture, temperature, and mineral N pools in boreal agricultural soils

Hem Raj Bhattarai · Maarit Liimatainen · Narasinha J. Shurpali · Perttu Virkajärvi · Hannu Nykänen · Marja Maljanen

Received: 30 March 2026 / Accepted: 23 July 2026

Abstract

Background and aims Reactive nitrogen gases (HONO, NO, N_2O) are key to atmospheric chemistry and climate forcing, yet their simultaneous *in-situ* emissions from boreal agricultural soils are poorly known. We aimed to quantify these gases during early crop growth, a period when emerging soil–plant interactions begin to shape soil microclimate and N cycling and to identify the main environmental and vegetation drivers controlling their fluxes.

Methods We quantified *in-situ* fluxes of HONO, NO, and N_2O simultaneously and key soil variables across oat, barley and bare-soil plots in eastern Finland. Further, we applied piecewise structural equation modelling (pSEM) to determine the direct and indirect effects environment and vegetation on gas emissions.

Results Daily emissions (μg N m^{-2} h^{-1}) were strongly dominated by N_2O (13.5–229), followed by NO (1.5–38.2) and HONO (1.0–13.0). Cumulative fluxes confirmed this hierarchy, with HONO ~ 9–11 times lower than N_2O and NO ~ 3 times lower than N_2O. pSEM showed that soil temperature and moisture were the main regulators, with HONO and NO emissions increasing with temperature and decreasing with moisture, while N_2O was driven solely by temperature.

Vegetation indirectly suppressed emissions by increasing soil moisture and lowering soil pH, which reduced nitrite and thus HONO and NO precursor availability, consistent with the lower mean NO fluxes from vegetated compared to bare soil surfaces (17.1 vs. 22.6 μg N m^{-2} h^{-1}).

Conclusion Our findings show that during early crop growth, soil–plant interactions are strongly shaped by physical drivers especially temperature and moisture which outweigh chemical controls.

Keywords Nitrogen gas emissions, nitrous acid · Nitric oxide · Nitrous oxide · Soil–plant interactions · Boreal agriculture

Responsible Editor: Xiaoxuan Su.

Supplementary Information The online version contains supplementary material available at https://doi.org/10.1007/s11104-026-08947-0.

H. R. Bhattarai (✉) · N. J. Shurpali · P. Virkajärvi
Natural Resources Institute Finland Luke, Halolantie 31, 71750 Maaninka, Finland
e-mail: hemraj.bhattarai@luke.fi

H. R. Bhattarai · M. Liimatainen · H. Nykänen · M. Maljanen
Department of Environmental and Biological Sciences, University of Eastern Finland, P.O. Box 1627, 70211 Kuopio, Finland

M. Liimatainen
Natural Resources Institute Finland Luke, Tutkimusasemantie 15, 92400 Ruukki, Finland

M. Liimatainen
University of Oulu, Pentti Kaiteran Katu 1, 90570 Oulu, Finland

Published online: 05 August 2026

Introduction

Agricultural soils can lose up to 5.8 Tg N yr^{-1} as nitrous oxide (N_2O) due to inefficient use of synthetic fertilizers, while mineralization and turnover of organic nitrogen (N) further contribute to N_2O production and emissions (Tian et al. 2020). N_2O emissions from agricultural soils pose three major risks: ozone depletion, climate warming, and reduced agricultural sustainability (Ravishankara et al. 2009). While the biogeochemistry of soil N_2O emissions is relatively well understood (Butterbach-Bahl et al. 2013; Zhu et al. 2025), knowledge of nitric oxide (NO) and nitrous acid (HONO) still remains limited (Pilegaard 2013; Su et al. 2011; Wang et al. 2025), despite their integral role in the soil N cycle and participation in key atmospheric reactions (Atkinson 2000; Kulmala and Petaja 2011).

Once emitted from soil, N_2O, NO, and HONO engage in key atmospheric reactions. N_2O contributes to climate warming and accelerates stratospheric O_3 depletion (Ravishankara et al. 2009). Similarly, NO promotes O_3 loss and facilitates formation of nitrate (NO_3^-) radicals, strong atmospheric oxidants alongside hydroxyl radicals (OH·) (Atkinson 2000). HONO photodissociation releases NO and OH·, the most reactive oxidant, which reduces CO and CH_4, both greenhouse gases and drives secondary organic aerosol and cloud formation, contributing to climate cooling (Claeys 2004; Lelieveld et al. 2016, 2004). Although the atmospheric relevance of N_2O, NO, and HONO is well recognized, their combined emission dynamics from soils remain poorly understood. These gases originate from mineral N cycling and share common substrates, ammonium (NH_4^+) and NO_3^-. In aerobic conditions, nitrification produces N_2O, NO, and HONO (Ermel et al. 2018; Oswald et al. 2013; Su et al. 2011) and provides nitrite (NO_2^-) — the HONO precursor ($NO_2^- + H^+ \rightleftharpoons HNO_{2(aq)} \rightleftharpoons HONO_g$) (Su et al. 2011). On the other hand, NO_3^- serves as a substrate for denitrification under anaerobic conditions and fuels the NO_2^- pool and thereby HONO emissions (Bhattarai et al. 2021; Wu et al. 2019). Also, unknown abiotic pathway other than acid–base reactions in soil can produce HONO (Bhattarai et al. 2021). Understanding these processes holistically is critical for agriculture, where mineral N fertilizer use is indispensable and projected to rise substantially by 2050 to meet global food and forage demand (FAO 2017; Wang et al. 2025; Zhu et al. 2025).

Emissions of reactive N-gases from soils are strongly controlled by substrate availability such as mineral N and labile carbon and soil physicochemical conditions including pH, moisture, and temperature, which regulate microbial processes responsible for N transformations (Butterbach-Bahl et al. 2013; Firestone and Davidson 1989; Firestone et al. 1979). Vegetation adds another layer of complexity by influencing these regulatory factors (Coskun et al. 2017; Kuzyakov 2002; Kuzyakov and Xu 2013; Nguyen 2003). Plants compete with nitrifiers and denitrifiers for mineral N, particularly NO_3^-, thereby altering substrate availability for N producing soil microbes (Kuzyakov and Xu 2013). Root activity modifies soil structure, porosity, and moisture, and can shift pH through rhizosphere processes (Hinsinger et al. 2009). Moreover, root exudates provide easily accessible C sources that stimulate microbial activity (Jones et al. 2004). These interactions can lead to substantial variation in N-gas emissions compared to bare soils, as shown previously (Bhattarai et al. 2022, 2019, 2018). Such vegetation-driven effects highlight the need to consider plant–soil interactions when assessing N_2O, NO, and HONO fluxes from agricultural systems.

Despite the atmospheric significance of HONO, NO, and N_2O, most previous studies have focused on unvegetated (i.e., bare) agricultural soils and relied on destructive sampling under laboratory-controlled conditions. This approach overlooks a key aspect: ground-truth, *in-situ* emission dynamics, which inherently include vegetation effects on N cycling—specifically plant competition for mineral N and the release of root exudates, including labile carbon. Simultaneous, *in-situ* measurements of HONO, NO, and N_2O from the same system is extremely rare, with only a few recent studies reporting such measurements under controlled conditions (Bhattarai et al. 2019, 2018; Cheng et al. 2025; Maljanen et al. 2018, 2016, 2023; Ndah et al. 2024; Song et al. 2024). To date, research has not addressed simultaneous *in-situ* emissions of these gases from boreal agricultural soils, even though such soils maintain persistent plant cover and receive substantial N fertilization in a short growing season. Boreal agricultural soils are seldom bare, as short growing season drive intensive cropping to meet forage and food demand, leaving only brief periods without vegetation. Given the competitive

nature of plants for mineral N and their role in providing fresh carbon inputs, understanding HONO, NO, and N_2O emissions under active vegetation is essential for improving mechanistic understanding and developing mitigation strategies for boreal agroecosystems. Therefore, this study aims to quantify the role of vegetation under *in-situ* conditions, especially during early growth phase (starting from germination) in regulating soil–atmosphere exchanges of reactive nitrogen gases (HONO, NO, and N_2O) and to evaluate how these fluxes are linked to vegetation-induced changes in soil physicochemical conditions arising from root–soil interactions and weather-driven dynamics.

To achieve this aim, we measured fluxes of HONO, NO, and N_2O during early vegetation growth phase (for 15-day after seeding) on a mineral agricultural soil in Eastern Finland with barley and oat as vegetated treatment and unvegetated surface (bare) as control. We refer to the 15-day period as the early growth phase because, during this period, the vegetation had reached the seedling stage, with root establishment and the emergence of the first true leaves, however had not yet entered the main tillering or more advanced vegetative growth stages. We choose this period because it has been shown to enhance mineral N transformation (e.g., $NO_3^- \rightarrow NO_2^-$) and emissions of N-gases in controlled conditions (Bhattarai et al. 2019). The study had two objectives: (i) to evaluate the effect of vegetation during their early growth phase on HONO, NO, and N_2O emission rates, hypothesizing that growing vegetation reduces emissions by competing with microbes for mineral N; and (ii) to examine associations between these emissions and changes in soil physicochemical variables and microclimate driven by vegetation, hypothesizing that vegetation induced changes influences soil conditions and microclimate thus emission dynamics.

Material and methods

Study site

The study was conducted in Maaninka, Eastern Finland (63° 09′ 49″ N, 27° 14′ 03″ E) on a mineral agricultural soil classified as Haplic Cambisol/Regosol (WRB). The topsoil is silt loam (USDA) with 5.2 ± 0.9% organic matter, 3.0 ± 0.52% organic C, 0.2 ± 0.03% total N, and a C:N ratio of 15 ± 0.4 (Lind et al. 2016). The region has an annual mean temperature (1981–2010) of 3.2 °C (− 9.4 °C in February; 17.0 °C in July) and annual precipitation of 612 mm, with 347 mm during the snow-free period (Pirinen 2012).

Study design and experimental plots

We conducted field measurement in experimental plots for 15 days in early summer (6–20 June) 2018. The experimental plots were established at the centre of a 6.3 ha field (Fig. S1) in Maaninka, Eastern Finland, adjacent (shadow-free) to a cabin providing power for analyzers and ~ 30 m from an eddy covariance tower measuring N_2O fluxes and meteorological parameters, air temperature (ºC) and precipitation (mm). To establish experimental plots, existing vegetation (*Phleum pratense* L.) was manually removed, the soil ploughed and crushed with a ploughing ripper, and remaining roots and plant material cleared by hand. Ten experimental plots (1 × 0.5 m, Fig. S1) were prepared and fenced on two sides with water-resistant plastic (0.15 m high) to prevent runoff and maintain uniform conditions. A wooden boardwalk was constructed on one edge along the plots to facilitate the movement of a metal trolley carrying measurement devices (Fig. S1).

As vegetation, we selected two cereals, barley (*Hordeum vulgare* L.) and oat (*Avena sativa* L.), crops that are suited for cold climate conditions. The experimental design consisted of three treatments: two vegetation treatments, "Barley" (*Hordeum vulgare* L.) and "Oat" (*Avena sativa* L.), and a non-vegetated control treatment ("Bare" soil). Each treatment was replicated three times, resulting in a total of nine experimental units (Fig. S1). The treatments were arranged sequentially: plot 1 was bare soil, plot 2 had oat, and plot 3 had barley, continuing in the same order across the experimental layout (Fig. S1). This design enabled direct comparison between vegetated and non-vegetated conditions, as well as between crop types, allowing assessment of plant–soil interactions and their influence on N-gas emissions. A day before gas flux measurements, we seeded (~ 14 g per plot) and fertilized (259 kg N ha^{-1}, Riedel de Haën, NH_4NO_3; purity > 99%) the plots, matching earlier laboratory study (Bhattarai et al. 2019). We installed PVC collars (h = 0.12 m, Ø 0.18 m) to half their

height to ensure stability and prevent gas leakage. The used barley seeds were fungicide-treated (Imazalil, 20 g L^{-1}; Cyproconazole, 5 g L^{-1}), while oats were untreated. We recorded soil temperature by placing temperature loggers (iButton®) at 5 cm depth in the centre of each plot, and air temperature was recorded from the eddy tower and nearby (~8 km) weather station operated by Natural Resources Institute Finland (Luke).

Gas flux measurement and calculations

To capture potential diurnal variation, surface fluxes of HONO, NO, and N_2O were measured consecutively across plots (1–9; Fig. S1) on each sampling day from 8:00 am to 16:00 pm following methods by Bhattarai et al., (2018, 2019). We measured HONO and NO fluxes using a dynamic chamber system connected to a LOPAP analyzer (QUMA Elektronik & Analytik GmbH, Germany; DL ≈ 3–9 ppt, flow 1 L min^{-1}, 10% relative error) (Heland et al. 2001; Kleffmann et al. 2002) and a NO_x analyzer (Thermo Fisher Scientific USA; DL ≈ 0.4 ± 0.2 ppb, flow 0.7 L min^{-1}). A 6 L PVC chamber lined (inner wall) with PTFE was flushed with pressurized and purified dry air (4 L min^{-1} or 4×10^3 cm^3 min^{-1}) during the measurements. Air was purified through activated carbon, Purafil® pellets, and HEPA filters and was pressurized using a commercial air compressor. The headspace HONO and NO concentrations were measured at the chamber outlet via Teflon tubing connected to analyzers. The Teflon tube was shielded with reflective material to prevent HONO photolysis. The background HONO and NO levels in the pressurized and purified dry air were checked every second by measuring bottom-sealed (via aluminium foil) empty PVC core prior to the plot measurements. We measured N_2O fluxes and ecosystem respiration by using a closed static chamber (6×10^3 cm^3 min^{-1}) on pre-installed PVC rings. The chamber headspace gas samples (25 mL) were collected at 5, 15, 25, 35, and 45 min after chamber enclosure using 60 mL syringes and injected immediately into pre-evacuated 12 mL vials (Labco Exetainers®, UK). The N_2O and CO_2 concentrations were analyzed with a gas chromatography (Agilent 7890B) equipped with an autosampler at the University of Eastern Finland. The flux rates (μg N m^{-2} h^{-1}) of HONO and NO were calculated using Eq. (1) whereas N_2O and CO_2 with Eq. (2) according to Bhattarai et al. (2018, 2019).

$$F1 = \frac{f_v}{1000} * \frac{1}{V_m} * \frac{T_0}{(T_0 + T)K} * \frac{p}{p_0} * \frac{\Delta c}{10^9} * \frac{60 * h * M}{A} * 10^6 \quad (1)$$

$$F2 = \frac{p_0 * k * V * M}{R * T * A} * 60 \quad (2)$$

In above equations, f_v is the purging flow rate (cm^3 min^{-1}), V_m is molar volume of the respective gas at the chamber temperature (l mol^{-1}), T_o is 273.15 K, T is temperature inside the chamber (K), p is air pressure (kPa), p_0 is 101.3 kPa, Δc is the concentration difference (ppb), k is slope of N_2O and CO_2 (ppm h^{-1}), V is the volume of the chamber headspace (m^3), R is the ideal gas constant (8.314 J k^{-1} mol^{-1}), M is the molar mass (g mol^{-1}) of the respective gases and A is the area of PVC collar (m^2).

Soil physiochemical properties and net nitrification rates

In addition to N-gas fluxes, we measured plant growth (via plant height), soil pH, electrical conductivity (EC), and mineral N concentrations (NO_2^-, NO_3^-, NH_4^+) in each plot. We measured plant height (cm) daily after germination using a measuring ruler. Soil samples (0–10 cm depth, Fig. S1) were collected every second day from the opposite end of the PVC collar in each plot (plots 1–9) using a metallic corer (Ø 3.5 cm). The collected samples were transported immediately to the laboratory at 4 °C for further analyses and the sampling spots were marked to avoid overlap soil sampling on subsequent days. In laboratory, Milli-Q H_2O and 1 M KCl extractions (1:5 w/v, soil:extractant) were performed to quantify NO_2^-, NO_3^-, and NH_4^+ concentrations following Bhattarai et al. (2018). The NO_2^- and NO_3^- concentrations were analyzed using ion chromatography (Thermo Scientific Dionex ICS-2100) coupled with an autosampler (AS-DV) whereas NH_4^+ was determined spectrophotometrically at 650 nm using the colorimetric method described by (Fawcett and Scott 1960). Soil pH and EC were measured from the same soil–water slurry prepared for NO_2^- and NO_3^- extractions. All extractions were performed every second day after sampling. The concentrations of NO_2^- and NO_3^- in water-extracts were analyzed immediately,

while KCl extracts were stored at 4 °C until analysis at the end of the field campaign. Soil moisture was measured daily after gas flux sampling at four points around each PVC core (~5 cm from the edge) using an ML3 ThetaProbe sensor. Readings (mV) from the probe were converted to gravimetric moisture content (GWC) using Eq. 3, where θ_v is volumetric moisture (%), ρ_w is water density (1 g cm^{-3}), and ρ_s is soil dry bulk density. The ρ_s was calculated as dry mass divided by fresh soil volume.

$$GWC(gg-1) = \theta_v * \frac{\rho_w}{\rho_S} \quad (3)$$

$$NNR = \frac{\left[(NO_3^- + NO_2^-) - N\right]_{ti} - \left[(NO_3^- + NO_2^-) - N\right]_{t0}}{\Delta t} \quad (4)$$

Net nitrification rates (NNR, μg NO_3^- g_{dw}^{-1} d^{-1}) were calculated using Eq. (4) as the change in nitrification products, defined here as the sum of soil NO_3^-–N and NO_2^-–N concentrations, day relative to the day 1 and divided by the elapsed time of the experiment. In Eq. (4), $\left[(NO_3^- + NO_2^-) - N\right]_{t_i}$ and $\left[(NO_3^- + NO_2^-) - N\right]_{t_0}$ represent the NO_3^-–N + NO_2^-–N concentrations on sampling day *i* and day 1, respectively, while Δt represents the time interval between sampling day *i* and day 1. This approach follows standard soil N-transformation methods in which net nitrification is estimated from the accumulation of oxidized inorganic N products over time, while inclusion of NO_2^- is justified because NO_2^- is an intermediate product of nitrification before oxidation to NO_3^- (Robertson et al. 1999; Robertson and Groffman 2015).

Statistical analysis

Time-series emissions and soil and plant data were analyzed using two-way mixed ANOVA (afex::aov_ez) (Singmann et al. 2012) with treatment and day as fixed factors and plot as a random factor. Normality and homogeneity were checked via QQ plots and Levene's test and sphericity were assessed with Mauchly's test and corrected using Greenhouse–Geisser when violated. Significant interactions were followed by Tukey-adjusted post-hoc tests. When normality assumptions failed, generalized linear mixed models (glmmTMB) with Gamma or Tweedie distributions (log link) were used. The Wald χ^2 tests (Type III) test was used to assess fixed-effect significance. Diagnostics were performed with DHARMa (Hartig 2016), and estimated marginal means (emmeans) (Searle et al. 1980) were back transformed when needed. However, we used Gaussian linear mixed model (lme4::lmer) (Bates et al. 2015) for soil pH to avoid double log transformation and checked model assumptions via residual diagnostics, and fixed effects were tested using Type III ANOVA (car::Anova) (Fox et al. 2001) and Tukey-adjusted contrasts were obtained with emmeans for post-hoc comparisons. Cumulative emissions and vegetation comparisons were analyzed using two-way and one-way ANOVA, respectively after $\log_{10}$ transformation, with assumptions checked via Shapiro–Wilk and Levene's tests. For cumulative emissions and mean emissions between vegetations Tukey-adjusted pairwise comparisons were made. When assumptions remained violated, Kruskal–Wallis tests were applied. Soil temperature was assessed using descriptive statistics, linear regression, and Kendall's rank correlation. All statistical test with $p < 0.05$ were considered significant. Correlations between total N-gas emissions and soil variables were examined using *corrplot* (Wei and Simko 2010). To elucidate vegetation effects on gaseous N emissions, we applied piecewise structural equation modeling using the *piecewise*SEM package in R (Lefcheck 2016) to data from vegetated plots (oat + barley), specifying a set of linear mixed-effects component models to quantify direct and indirect pathways among soil variables and N-gas fluxes. Prior to modeling, soil predictors were standardized and for each component model we assessed residual normality (QQ plots), multicollinearity, and model adequacy, and evaluated the integrated SEM fit with Fisher's C and d-separation tests to validate the hypothesized causal graph (Shipley 2000). All analyses were conducted in R (v4.5.2).

Results

Daily and cumulative emissions

The daily fluxes of HONO, NO, and N_2O in terms of N (μg N m^{-2} h^{-1}) were consistently positive, indicating net soil emissions, with N_2O dominating, followed by NO and HONO across all treatments (Fig. 1a).

Both gases showed strong day effects (HONO: Type-III Wald $\chi^2(11) = 86.70$, $p < 0.001$, joint-tests

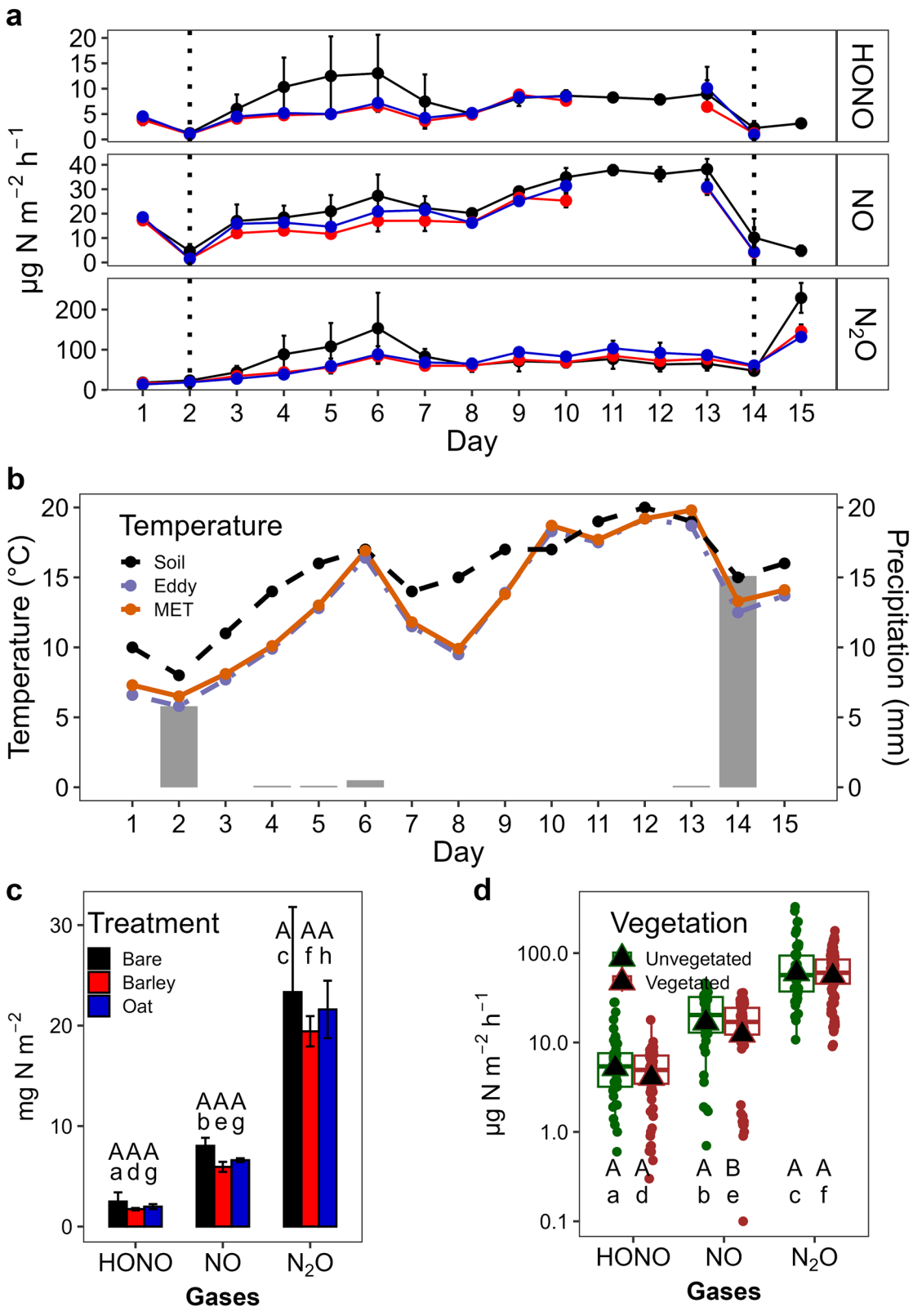
a
HONO
NO
N2O
μg N m−2 h−1
Day
b
Temperature
Soil
Eddy
MET
Temperature (°C)
Precipitation (mm)
Day
c
Treatment
Bare
Barley
Oat
mg N m−2
AAA a d g
AAA b e g
A c
AA f h
HONO
NO
N2O
Gases
d
Vegetation
Unvegetated
Vegetated
μg N m−2 h−1
A a
A d
A b
B e
A c
A f
HONO
NO
N2O
Gases

◂**Fig. 1** Daily fluxes, cumulative emissions of HONO, NO, and N_2O and climatic conditions. Plots: a, daily mean emission rates (μg N m^{-2} h^{-1}); b, daily soil and air temperature (ºC) and precipitations (mm as bars); c, mean cumulative emissions (mg N m^{-2}) over 14 days; d, emission rates (μg N m^{-2} h^{-2}) from vegetated (barley + oat) and bare plots. Colours in plots a and c represents experimental treatments—bare (black), barley (red), oat (blue); b represents—soil temperature (black line), air temperature (orange from eddy tower and violet from meteorological station), grey (precipitation) and in plot d represent vegetation—vegetated (brown), bare (green). In a and b, dots and error bars show mean ± SE (n = 3) whereas boxes in plot c show median (central black line), interquartile ranges (IQR), lower (1.5 × IQR as minimum) and upper whiskers (75th percentile + 1.5 × IQR as maximum) and mean emissions (black solid triangles). Two dotted lines in plot a mark two precipitation events on corresponding days. Note: Plot a uses different y-axis scales per gas; c uses $\log_{10}$ scale on y-axis. In plots c and d, capital letters indicate significant differences ($p < 0.05$) among treatments and between vegetation, while lowercase letters show differences among gases within each treatment and vegetation group

$F = 28.48$; NO: $\chi^2(11) = 86.14$, $p < 0.001$; joint-tests $F = 0.94$), with no overall treatment and interaction effect. The HONO emission on day 2 was much lower than day 1 (Bare $p = 0.020$, Barley $p = 0.0005$, Oat $p < 0.0001$) and significantly lower than most subsequent days ($p < 0.001$). Emissions increased through the mid-period (days 4–13) and then declined by day 14, with mid-period days being higher than day 14 in all treatments ($p < 0.01$, Fig. 1a). Similarly, NO emission was very low on day 2 (~2.2 μg N m^{-2} h^{-1}) and peaked on days 10–13 (~30–33 μg N m^{-2} h^{-1}). Within treatments, NO emissions varied markedly over time. In bare plots, day 2 NO emission was lower than day 1 ($p = 0.004$) and days 10–13 ($p < 0.001$). In barley and oat plots, day 2 NO emission was lower than day 1 and late days (days 10–14; $p < 0.001$). These results indicate that HONO and NO emissions are broadly similar across treatments, with bare soil generally exhibiting the highest emissions. Their emission pattern largely reflected by temperature dynamics, rising during the mid-period and declining toward day 14 and further by soil moisture change, with reduced fluxes during rain events on days 2 and 14 (Fig. 1a–b). Despite these shared effects, HONO and NO emissions showed a distinct temporal emission dynamic. HONO showed an earlier, sustained increase, whereas NO exhibited more pronounced late peaks. Effect size estimates (large day χ^2 and joint-test F values versus small treatment effects) confirm that temporal dynamics were the primary driver for both gases. The daily mean HONO emissions ranged from 1.23–13.0, 1.1–10.1 and 1.0–8.8 μg N m^{-2} h^{-1} while NO ranged from 4.6–38.2, 1.5–31.4 and 1.5–30.5 μg N m^{-2} h^{-1} for bare, oat and barely, respectively (Fig. 1a and Table S1).

The daily N_2O emissions varied significantly across days ($F_{14,84} = 49.38$, $p < 0.001$) whereas effect of treatment remained insignificant. Post hoc comparisons confirmed strong day-to-day shifts in all treatments. In bare plots, emissions rose significantly after day 1, with higher values on days 5–13 ($p \leq 0.045$), a temporary dip on day 14 ($p = 0.042$), and a sharp peak on day 15 ($p < 0.001$). Barley and oat followed a similar pattern, day 1 was lower than days 6–15 (barley: $p \leq 0.031$; oat: $p \leq 0.0185$), and day 14 was lower than day 15 (barley: $p = 0.012$; oat: $p = 0.0256$). Overall, emissions showed an early increase, a mid-period plateau, a late dip, and a final rebound across all treatments. The N_2O emissions were initially low in all treatments which contrasts with HONO and NO emissions. The daily mean N_2O emissions ranged from 18.1–229.0, 13.5–131.7 and 16.9–145.6 μg N m^{-2} h^{-1} for bare, oat and barely, respectively (Fig. 1a and Table S1).

The cumulative emissions (mg N m^{-2}) varied significantly ($F_{2,18} = 128.82$, $p < 0.001$) between gases in each treatment, however not among treatments nor their interactions (Fig. 1b and Table S2). In all treatments, cumulative emissions between gases were significant ($p < 0.001$) and followed the order $N_2O > NO > HONO$. Compared to N_2O, cumulative NO emissions were 2.9 times lower in bare soil and 3.2 times lower in barley and oat, while HONO was 9.4 times lower in bare and ~ 11.2 times lower in both, oat and barley. HONO was also about 3.2 times lower than NO across treatments. We found a significant difference between gas emissions ($F_{2,363} = 338.5$, $p < 0.001$) when vegetated and bare soil surfaces were compared (Fig. 1c). This effect of vegetation was significant ($p = 0.027$) only for mean NO emission rates, not for HONO and N_2O. The mean NO emissions rates were higher in bare (22.6 μg N m^{-2} h^{-1}) than vegetated (17.1 μg N m^{-2} h^{-1}) surfaces (Fig. 1c and Table S3).

Changes in soil temperature, vegetation, moisture and pH

Soil temperature increased steadily over the 15-day period, ranging from 8 ºC on day 2 to 20 ºC on day 12 (Fig. 1b). Linear regression indicated a significant upward trend (slope = 0.57 ºC day^{-1}, $R^2 = 0.56$,

$p=0.0013$) with a monotonic increase ($\tau=0.59$, $p=0.0027$). Oat and barley germinated within six days (Fig. 2a), and their heights showed a significant interaction (days × treatment) ($F_{8,32}=3.84$, $p=0.003$) effect. The differences between plant height emerged from day 10 onwards when barley exceeded oat, especially on day 10 ($p=0.032$), day 14 ($p=0.024$), and day 15 ($p=0.022$) while early comparisons (days 7–9) were mostly non-significant. The mean plant height also varied; it was significantly higher in barley than oats (Fig. 2a).

Soil moisture (GWC; $\chi^2=531.84$, df = 14, $p<0.001$, Fig. 2b) and soil pH ($\chi^2=83.14$, df = 13, $p<0.001$, Fig. S2) showed stronger temporal than treatment variations. Within each treatment, soil moisture showed a consistent temporal trend with two sharp rises, one on

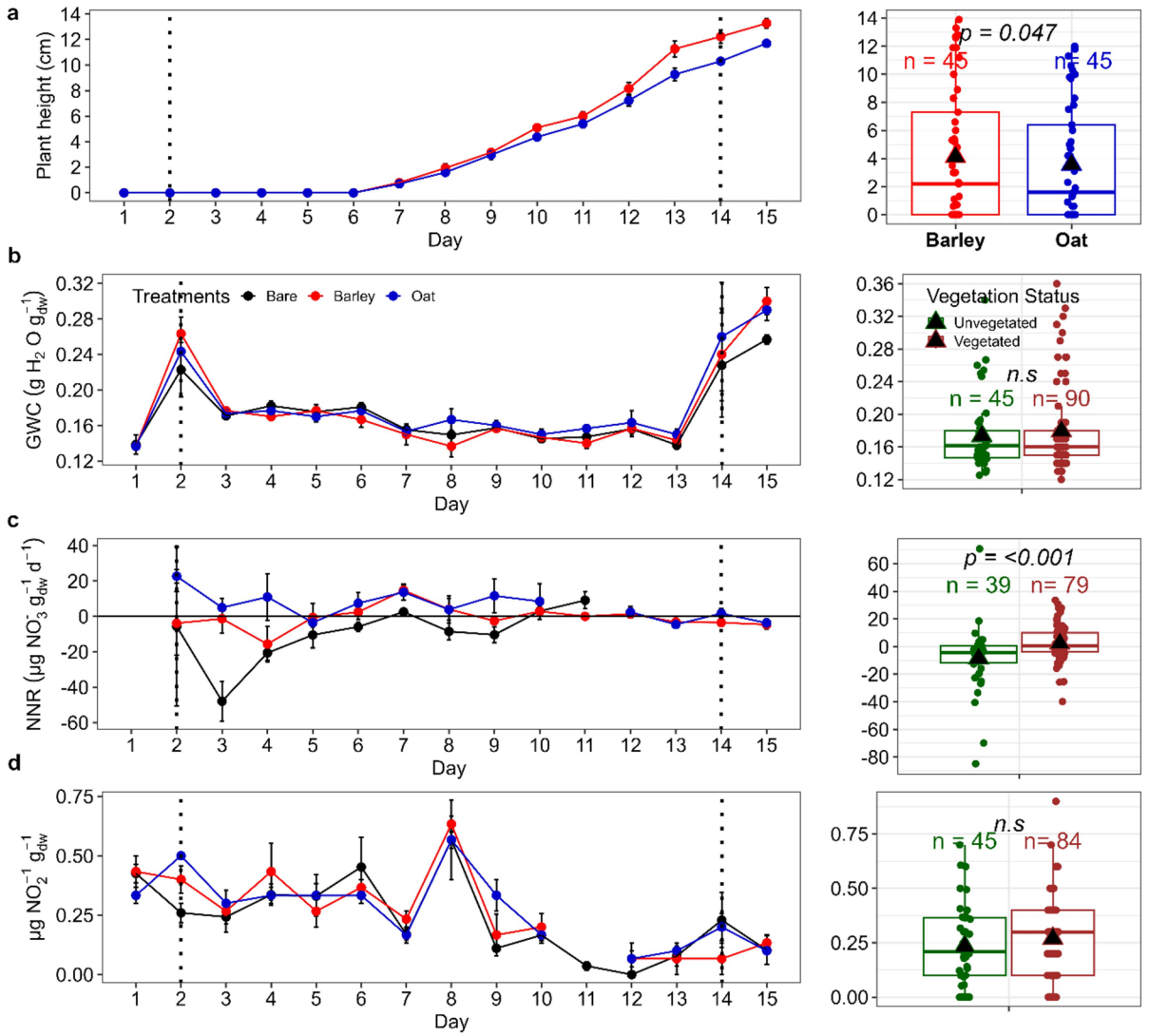

Fig. 2 Soil and plant properties during experimental period. Plots: a, plant height (cm); b, gravimetric moisture content (GWC, g H_2O g_{dw}^{-1}); c, net nitrification rates (NNR, µg NO_3^- $g_{dw}^{-1}d^{-1}$), and d, soil nitrite concentrations (µg N g_{dw}^{-1}). Colors in plots a-d represents experimental treatments; bare (black), barley (red), oat (blue). The box plots on the right summarize the same variables grouped as vegetated (barley + oat, brown) and bare (green). Points and error bars indicate means ± SE (n = 3). The box plots show median (central black line), interquartile ranges (IQR), lower (1.5 × IQR as minimum) and upper whiskers (75th percentile + 1.5 × IQR as maximum), mean (triangle) and total number (n) of observations. Two dotted lines in each plot mark two precipitation events on corresponding days

early period (day 2) and another on late period (days 14–15) aligning with precipitation events. Soil moisture increased sharply on day 2 compared to day 1 ($p<0.01$) across all treatments and remained significantly higher than mid-period soil moisture (days 7–13 in Bare; days 3–13 in Barley and Oat). Soil moisture declined gradually across all treatments after day 2 until second sharp rise on days 14–15, which also exceeded early and mid-period levels ($p<0.01$). Soil pH shows an initial rise until day 4, after which it decreased steadily until day 13 followed by an increasing trend until day 15. However, this trend for most day-to-day differences remained non-significant across all treatments except barley. In Barley plots, pH was significantly higher on day 4 compared to days 7, 12, and 15 ($p<0.05$). Both, soil moisture and pH remained non-significant between bare and vegetated (barley + oat) surfaces.

Net nitrification and mineral nitrogen dynamics

The NNR or net NO_3^- production ($\chi^2=46.59$, df = 12, $p<0.001$, Fig. 2c), NO_2^- concentrations ($\chi^2=170.83$, df = 13, $p<0.001$, Fig. 2d), NO_3^- concentrations ($F_{13,78}=2.84$, $p=0.002$, Fig. S2), and NH_4^+ concentrations ($F_{13,78}=1.95$, $p=0.036$, Fig. S2) showed strong temporal than treatment variations except NNR which showed also treatment effect ($\chi^2=7.11$, df = 2, $p=0.029$).

In general, NNR showed an early peak followed by a pronounced late reduction that was uniform across treatments. When averaged over days, oat showed a ~ 5.5-fold higher ($p=0.021$) NNR compared to bare while other treatment differences were insignificant. Within treatment, NNR revealed a consistent pattern across days where day 2 exhibited the highest NNR, significantly ($p<0.05$) higher than late-period, especially day 5 and days 14–15 NNR. Although non-significant, on day 3, a day after the moisture peak, the bare treatment exhibited greater net NO_3^- consumption than production, contrasting with the patterns observed in the oat and barley treatments.

Soil NO_2^- concentrations exhibited a consistent temporal pattern across all treatments showing a gradual decline over 15-days period. Until day 6, soil NO_2^- concentrations remained relatively stable and insignificant across treatments although there were some variations. On day 7, it decreased significantly (vs. days 1–2 and day 6, $p<0.05$) and then increased sharply on day 8, two-days after seed germination, which was significantly higher than many early (days 1, 3 and 7, $p<0.05$) and all late days (days 9–15, $p<0.05$). After Day 8, NO_2^- concentrations declined steadily further toward the end of the measurement period. However, there was a slight increase in NO_2^- concentrations on the second precipitation event (day 14) which was comparable to few early high NO_2^- concentrations days (days 3, 5 and 7).

Overall, soil NO_3^- and NH_4^+ concentrations across treatments (Fig. S2) followed a broadly similar trend from day 3 onward, showing a gradual increase until day 11 with temporary declines on days 8 and 9. In contrast, the first three days exhibited distinct patterns, NH_4^+ concentrations increased on day 2 before dropping sharply on day 3, whereas NO_3^- remained similar between days 1 and 2 and then declined markedly on day 3 across all treatments. The increasing NO_3^- concentrations after day 3 were significant only for bare plots (not barley and oat) only on few occasions. Bare plots showed significantly higher NO_3^- concentrations on day 3 than day 1 ($p=0.028$) and further increases on days 5 and 7 compared to day 3 ($p<0.05$), while other contrasts were non-significant. For NH_4^+, most contrasts were non-significant; only oat plots showed higher NH_4^+ concentrations on day 7 than day 1 ($p=0.029$).

When bare and vegetated (barley + oat) groups were compared, only NNR ($\chi^2=16.53$, df = 1, $p<0.001$) showed a significant difference, indicating that vegetation status affected NNR, it was higher in vegetated than bare plots. This effect likely contributed from oat treatment as it showed higher NNR (5.5 folds) compared to barley.

Ecosystem respiration

The ecosystem respiration (CO_2 emissions in the dark chamber) varied significantly across days ($F_{14,84}=30.71$, $p<0.001$), among treatments ($F_{2,6}=6.41$, $p=0.032$) and interactions (treatment × day; $F_{28,84}=8.76$, $p<0.001$) indicating that temporal patterns of CO_2 emissions were treatment dependent (Fig. S2). The CO_2 emissions showed a gradual increase with time, especially in barley and oat while contrasting pattern was seen in bare treatments. The difference in CO_2 emissions between treatments start to emerge from day 8 onward, where barley and oat consistently showed higher CO_2 emissions than bare, with strong significance ($p<0.001$) on days 8, 10–14. On day 15, CO_2 emissions were significantly

higher ($p=0.035$) only in Barley (not oat) compared to bare. Barley and oat did not differ significantly throughout the period except on day 5, where oat showed significantly ($p=0.026$) lower CO_2 emissions than barley. The CO_2 emissions showed a significant difference ($F_{1,133}=20.12$, $p<0.001$) between vegetation status, it was higher in vegetated than bare plots.

Effects of precipitation on emission rates

Rainfall events caused pronounced shifts in HONO, NO, and N_2O emissions. Both HONO and NO emissions declined on both, the first low (day 2) and second high (day 14) precipitation events, whereas N_2O emissions increased on the first and decreased on the second (Figs. 1 and 3). Although reductions were generally similar among treatments, differences emerged between gases. During the first event, mean NO emissions decreased by 92%, significantly more than HONO reductions (72–77%) in barley and oat ($p<0.05$). In contrast, mean N_2O emissions increased by 18–46% across treatments, a significant rise compared to HONO and NO reductions ($p<0.05$). During the second event, mean NO reduction (83%) exceeded N_2O reduction (28%) only in oat ($p<0.05$), while other differences among gases and treatments were statistically nonsignificant. These patterns highlight contrasting gas-specific responses to rainfall, with N_2O exhibiting both resilience or even stimulation under conditions that suppressed HONO and NO.

While the above describes the immediate impact of rainfall on the day it occurred, its effects on subsequent N-gas emissions are also distinctive. Both HONO and NO showed similar responses after rainfall, particularly following the first event, though patterns varied among treatments (Fig. 1a–b). After the initial smaller rainfall (6 mm day^{-1}), HONO emission increased sharply in bare soil on days 5–7, whereas barley and oat treatments exhibited a gradual increase. In contrast, NO emissions showed a steady increase across all treatments during the same period. Following the second rainfall, an opposite trend emerged. HONO emission displayed an upward trajectory, while NO emission declined (day 15 vs. day 14, Fig. 1a–b). This pattern, although mainly in bare soil (oat and barley were not measured), suggests that NO is more sensitive to moisture than HONO and supports the greater reduction of NO during the first rainfall compared to HONO. N_2O responded differently than HONO and NO after the rainfall events, especially after the higher second rainfall event. After the first rainfall, N_2O emissions increased steadily until day six across all treatments, then rose sharply after the second rainfall, peaking at 229.0 μg N m^{-2} h^{-1} in bare soil, 145.6 μg N m^{-2} h^{-1} in barley, and 131.7 μg N m^{-2} h^{-1} in oat. These patterns highlight contrasting gas-specific responses after the rainfall period likely due to changes caused by precipitation to soil moisture and interactions with vegetations.

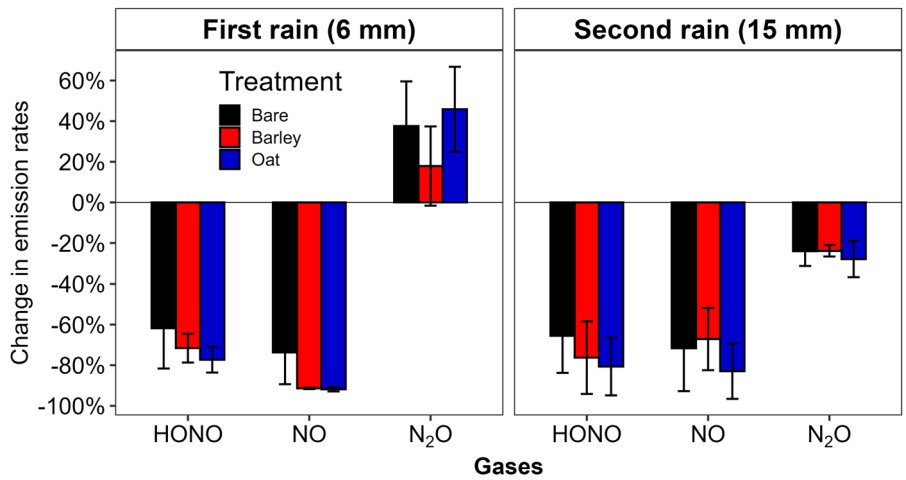

Fig. 3 Percentage (%) change in HONO, NO, and N_2O emission rates following two rainfall events. The left panel represent the first event (6 mm on day 2), and the right panel the second event (15 mm on day 14). Positive values indicate increased emissions compared to the day before rainfall, while negative values indicate reductions

Association between N-gas emissions and soil and plant variables

Associations between N-gas emissions and soil variables were more pronounced in vegetated plots than in bare soil (Fig. 4). Under vegetation, HONO fluxes showed strong positive association with NO, soil temperature, and N_2O emissions, and moderate positive links with CO_2 emissions. NO exhibited similar positive associations with soil temperature, N_2O, and CO_2 emissions. N_2O emissions were most strongly associated with soil temperature followed by CO_2 emissions, and plant height. In contrast, HONO and NO were negatively associated with soil moisture, with NO showing a stronger negative relationship. N_2O displayed a moderate negative association with soil NO_2^- concentration. Soil NO_2^- itself was moderately negatively correlated with plant height, CO_2, N_2O and NO emissions, and soil temperature, however positively associated with soil pH. Soil pH on the other hand showed moderate negative links with plant height, NH_4^+ and NO_3^- concentrations and electrical conductivity. Soil moisture showed a moderate negative link with soil temperature. These patterns indicate that vegetation amplifies interactions among gas fluxes and soil physiochemical properties, particularly temperature and plant growth, while moisture and NO_2^- exert contrasting controls.

In the absence of vegetation, HONO emissions were strongly associated with NO and moderately with N_2O, however showed no significant links to soil variables. NO emissions exhibited a moderate negative correlation with soil moisture and a strong positive correlation with soil temperature. N_2O emissions were positively associated with CO_2 emissions and weakly with soil moisture. Soil NO_2^- showed a moderate negative relationship with soil temperature and a moderately strong positive association with soil pH. Both NO_3^- and NH_4^+ displayed positive associations, though these were notably stronger in vegetated soils compared to bare plots. These patterns suggest that vegetation absence reduces the complexity of gas–soil interactions, leaving temperature and moisture as the primary drivers for NO and N_2O fluxes.

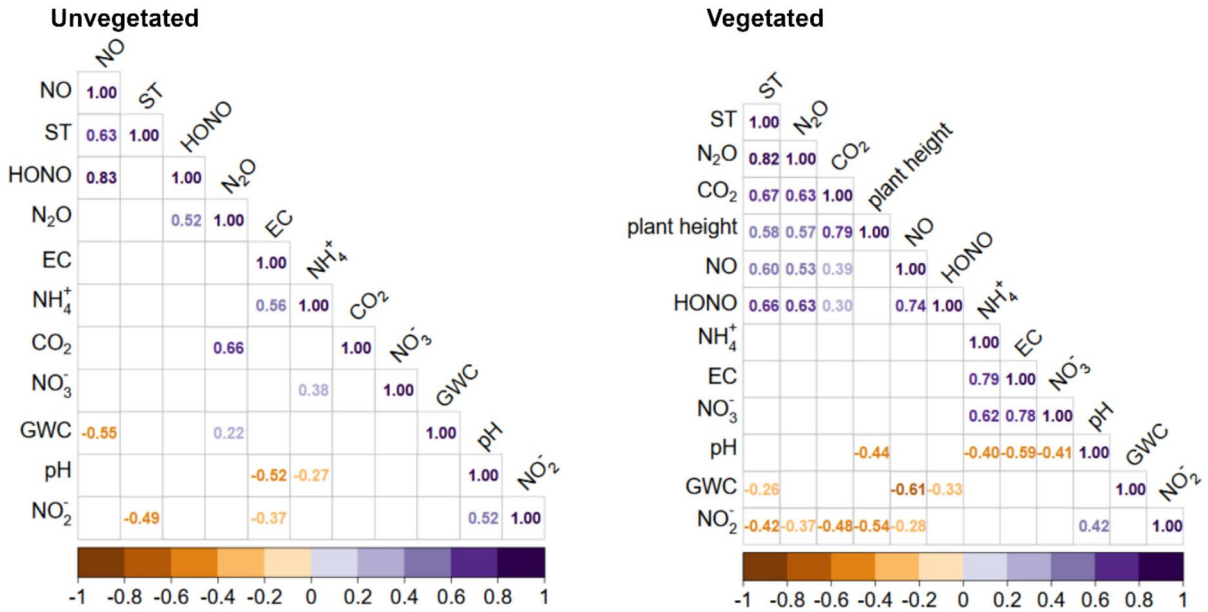

Fig. 4 Associations between HONO, NO, and N_2O emissions and soil–plant variables in bare (left) and vegetated (right) soils. Acronyms: ST = soil temperature (°C), GWC = gravimetric water content (g H_2O g^{-1} dw), EC = electrical conductivity (µmol S^{-1}), NH_4^+ = ammonium (µg N g^{-1} dw), NO_3^- = nitrate (µg N g^{-1} dw), NO_2^- = nitrite (µg N g^{-1} dw), CO_2 = CO_2 flux (mg C m^{-2} h^{-1}). Numbers in boxes indicate the strength of association, with the sign denoting direction: positive for similar trends and negative for opposite trends. Only statistically significant associations (* $p < 0.05$) are shown

Role of vegetation: Insights from piecewise SEM

Piecewise structural equation modelling revealed distinct yet interconnected controls on HONO, NO, and N_2O emissions under boreal conditions. Across gases (Fig. 5), physical constraints dominated during the early season, while rhizosphere chemistry exerted secondary, mediated influences. Model fit was excellent for HONO (Fisher's C = 1.61, df = 6, p = 0.95), NO (Fisher's C = 2.02, df = 6, p = 0.92) and N_2O emissions (Fisher's C = 2.21, df = 6, p = 0.90).

HONO emissions were primarily controlled by soil temperature and moisture. Soil temperature had a strong direct positive effect (β = +0.60, p < 0.001) and an additional indirect positive effect (≈ +0.19) via its negative impact on soil moisture (Temperature → Moisture = –0.541), yielding a total temperature effect ≈ +0.79. Soil moisture exerted a strong direct negative effect (β = –0.35, p < 0.001). Plant height (proxy for vegetation) showed a negative total effect (≈ –0.35), dominated by its indirect path through moisture (Plant height → Moisture = +0.433; indirect ≈ –0.12), while its direct effect was modest (β = –0.22, p = 0.057).

NO emissions followed similar patterns however with contrasting strengths. Soil moisture exerted the strongest direct negative effect (β = –0.60, p < 0.001), while soil temperature had a moderate positive direct effect (β = +0.37, p < 0.001). Temperature also contributed an indirect positive effect (≈ +0.35) via moisture, giving a total temperature effect ≈ +0.72, compared to moisture's total effect of –0.60. Plant height had a negative total effect (≈ –0.19), primarily through its influence on moisture (indirect ≈ –0.14). Direct effects of pH, NO_3^-, NH_4^+, and NO_2^- on HONO and NO were non-significant, and their indirect contributions remained minor compared to the dominant impacts of soil temperature and moisture.

In contrast, N_2O emissions were controlled almost exclusively by soil temperature (β = +0.89, p < 0.001), with no significant direct effects of moisture, pH, NO_3^-, NH_4^+, or plant height.

The mediator network was consistent across gases: soil moisture declined with rising temperature (β = –0.54, p < 0.001) and increased with plant height (β = +0.43, p < 0.001); soil pH decreased with plant height (β = –0.41, p < 0.001), NO_3^- (β = –0.42, p < 0.001), and NH_4^+ (β = –0.26, p < 0.05). Mineral N coupling was strong (NH_4^+ → NO_3^-: β = +0.53, p < 0.001), and NO_2^- increased with soil pH (β = +0.32, p < 0.01) and NO_3^- (β = +0.34, p < 0.01) however decreased with plant height (β = –0.30,

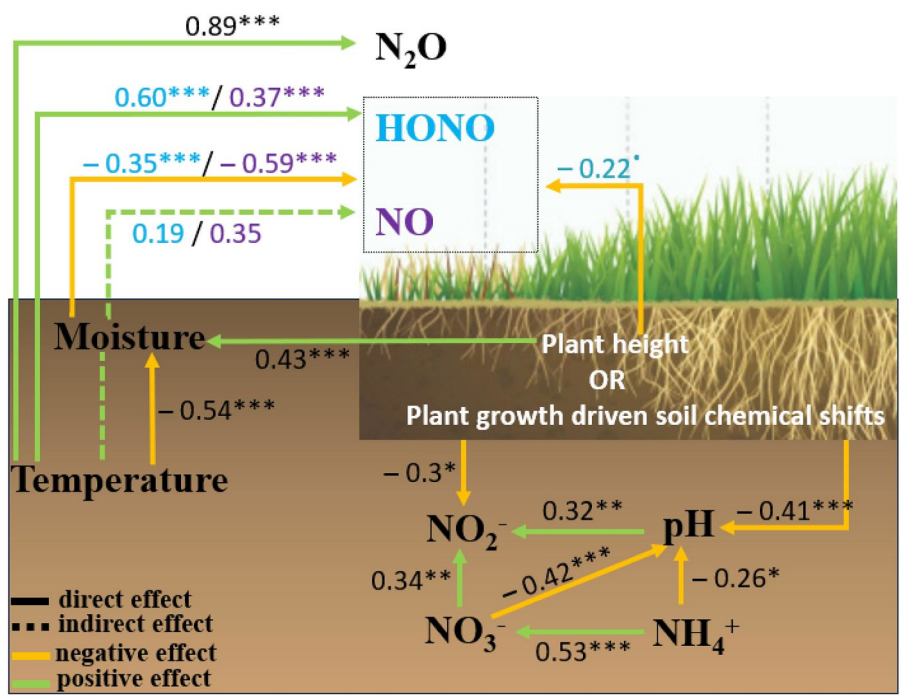

Fig. 5 Conceptual framework from piecewise SEM showing shared network of physical constraints and plant induced soil chemical shifts for HONO, NO, and N_2O emissions. The solid and dotted lines indicate direct and indirect effects, respectively and yellow and green lines represent negative and positive effects, respectively. Values on arrows are standardized coefficients with significance (*** p < 0.001; ** p < 0.01; * p < 0.05; • p < 0.10). Acronyms are, NO_2^- = nitrite, NO_3^- = nitrate, NH_4^+ = ammonium, and soil pH

$p < 0.05$). Model explanatory power was highest for NO and N_2O ($R^2_m = 0.67$) and moderate for HONO ($R^2_m = 0.52$).

Discussion

Our study provides the first simultaneous *in-situ* measurements of HONO, NO, and N_2O from Finland, representing boreal agricultural soils, and confirms that these soils are active sources of all three gases (Fig. 1). Importantly, this is the first report of concurrent *in-situ* emissions of HONO, NO, and N_2O from boreal mineral agricultural soils. Previous work has either documented all three gases under controlled laboratory conditions (Bhattarai et al. 2019, 2018; Maljanen et al. 2013) or reported concurrent emissions pairing NO and N_2O only, primarily from organic soils (Koponen et al. 2006; Regina et al. 1998a, b) and, to a lesser extent, from mineral soils (Maljanen et al. 2007).

N_2O as the dominant emission, followed by NO and HONO

Our study shows that *in-situ* emissions of N-gases are dominated by N_2O, followed by NO and HONO regardless of crop types (oat vs. barley) and presence of vegetation (bare vs. vegetation) (Fig. 1, Tables S2—4). This hierarchy of N-gas emissions agrees with previous studies on boreal soils that have either addressed all three gases on grassland (Bhattarai et al. 2018), wheat (Bhattarai et al. 2019) and cultivated peat soil (Maljanen et al. 2013) or in pairing NO and N_2O on peatland forest (Regina et al. 1998a, ba, b, 1998a, ba, b) and grassland (Maljanen et al. 2007) except to those of boreal afforested soils that showed higher NO than N_2O, especially at lower temperatures (Koponen et al. 2006). These findings are consistent with studies across various crops and climate zones. For example, research in subtropical regions reported higher NO than HONO emissions under diverse agricultural practices, with emissions strongly influenced by precipitation, temperature, and fertilization (Meng et al. 2024; Tang et al. 2020). Similarly, fertilized winter wheat fields showed greater N_2O than NO emissions, with patterns shaped by soil moisture and fertilizer N input (Gao et al. 2018). Long-term measurements in the North China Plain confirmed higher NO than HONO emissions from maize and wheat, driven by mineral N availability (Song et al. 2024). Overall, these studies suggest that the hierarchy of N-gas emissions is largely independent of crop or soil type however strongly controlled by environmental factors and N cycling processes, particularly moisture regimes, fertilization events, and NO_2^- dynamics (Cheng et al. 2025; Song et al. 2024).

Negligible effects of treatment on emissions of all N-gases

Total HONO, NO and N_2O emissions did not differ among treatments, despite marginal within-period fluctuations and higher variability in bare soil (Fig. 1). Statistics indicated only temporal effects, with no main treatment effect or treatment × time interaction, implying that vegetation presence per se had little influence during the campaign. The absence of strong treatment effects likely reflects the combined influence of short experimental duration, limited vegetation biomass accumulation, competing rhizosphere processes, and overriding physical controls, especially soil temperature and moisture.

We found that air temperature increased steadily (0.57 °C Day^{-1}) alongside soil temperature (Fig. 1b), suggesting temperature-driven processes masked vegetation impacts. This overriding effect of temperature is consistent with existing knowledge about temperature-sensitive N transformations masking subtle vegetation signals (Firestone and Davidson 1989; Butterbach-Bahl et al. 2013), which especially valid for vegetation that are at their early growth phases like in our study.

Mechanistically, warming accelerates nitrifier and denitrifier activity, increases substrate turnover ($NH_4^+ \rightarrow NO_2^-/NO_3^-$ and $NO_3^- \rightarrow NO/N_2O$), and enhances microbial respiration, collectively elevating baseline N-gas production (Butterbach-Bahl et al. 2013). At the same time, moisture-driven diffusional limits and pH-sensitive NO_2^- chemistry constrain HONO and NO emissions more than N_2O, allowing abiotic controls to overshadow short-term vegetation effects (Linn and Doran 1984; Oswald et al. 2013; Scharko et al. 2015). We nevertheless observed vegetation contrasts relevant to N cycling. Barley, relative to oat, is associated with higher-molecular-weight exudates and more robust rhizosheaths, which strengthen root–soil contact and can promote mineralisation and nutrient acquisition (Galloway et al. 2022; Lu et al. 2020). In line with this,

barley reached greater height (Fig. 2a) and often showed higher CO_2 emissions (Fig. S2), indicating stronger C inputs and microbial stimulation. Yet such rhizosphere priming (Kuzyakov 2010, 2002) did not translate into direct and discernible HONO, NO, or N_2O responses, likely because early growth phases deliver modest, patchy C exudation and the monotonic warming and near-surface microclimate exerted first-order control on net emissions (Davidson 1993; Pilegaard 2013). Also, due to short measurement period (15-day), plant-driven changes in mineral N demand, rhizosphere C supply, and soil microclimate may not yet have accumulated sufficiently to produce strong treatment-level differences. Although root exudates during early growth can stimulate microbial activity and N transformations, this stimulation may have been partly offset by plant–microbe competition for mineral N, particularly under fertilized conditions. These results accord with recent *in-situ* studies showing that management (fertiliser placement, irrigation, tillage) and microclimate explain seasonal HONO, NO and N_2O budgets better than plant presence alone (Song et al. 2024; Meng et al. 2024). This interpretation is further supported by piecewise analysis for vegetated soils, which identified physical constraints, soil temperature, and moisture as primary regulators of emissions rather than vegetation (Fig. 5).

Soil temperature promotes the emissions of all three N-gases

The SEM results demonstrate that HONO, NO and N_2O emissions during early stages of vegetation growth in boreal agricultural soils are primarily controlled by microclimatic factors, particularly temperature and moisture (see more details below) rather than direct influences from mineral N pools and vegetation (see more details below).

The strongest positive effect on HONO was from temperature, both directly (+0.60) and indirectly (+0.19 via reduced soil moisture), implying that HONO emissions are higher at higher soil temperatures. This supports previous findings that warmer, drier soils enhance HONO release by favouring NO_2^- accumulation and abiotic release pathways (Bhattarai et al. 2021; Oswald et al. 2013; Song et al. 2024, 2023; Wu et al. 2019, 2019). This effect could primarily link with thermal acceleration of NO_2^-chemistry, enhanced gas-phase diffusion under drier conditions and NO_2^- producing microbial process.

An enhanced abiotic desorption and volatilization from surface NO_2^- reservoirs could be expected as thermal energy increases increasing diffusional transport of HONO from near-surface reaction sites to the atmosphere (Su et al. 2011). Additionally, temperature-accelerated microbial turnover that may refresh near-surface NO_2^- pools even if bulk NO_2^-does not rise to predictive levels, again increasing HONO emissions. Although, HONO formation depends on the equilibrium between aqueous phase HONO and NO_2^- ($HNO_2 \rightleftharpoons NO_2^- + H^+$), making it sensitive to pH and NO_2^- pools, however these chemical factors contributed only minor indirect effects compared to temperature and moisture constraints. For boreal soils, we previously have shown that seed germination stimulates NO_2^- production (Bhattarai et al. 2019) and that denitrification serves as a major HONO source by enhancing NO_2^- accumulation (Bhattarai et al. 2021). Consistent with this, we observed a marked increase in soil NO_2^- concentrations during the germination phase (see peak on day 8, Fig. 2d). Although not statistically significant, the mean NO_2^- levels were slightly higher in vegetated surfaces compared to bare soil (0.27 vs. 0.23 μg N gdw^{-1}, Fig. 2d), with NO_3^- rather than NH_4^+ contributing to the NO_2^- pool in vegetated soils (Fig. 5), an indication that of active denitrification fuelling HONO precursor, i.e., the NO_2^- pool at our study site. Nevertheless, the absence of detectable direct effects from NO_3^-, NO_2^- or pH on HONO during early growth of vegetation suggests that release and transport constraints (e.g., thermal desorption, gas-phase diffusion, boundary-layer exchange) outweighed substrate supply constraints. This further aligns with the observed network of N transformations where NH_4^+ oxidation to NO_3^- was strong, NO_3^- (and NH_4^+) lowered pH, and pH together with NO_3^- increased NO_2^- (Fig. 5). However, this biogeochemical transformation did not translate into a direct effect controlling HONO emissions, implying that the bottleneck for HONO emission under early growth was not the formation of NO_2^- per se however the efficiency of transfer from reaction sites to the air column, a process that scale positively with temperature.

Similarly, strongest positive effect on NO emissions was also from temperature, both directly (+0.37) and indirectly (+0.35 via reduced soil moisture), implying that NO emissions increase with increasing soil temperatures. This result agrees with previous both

field and laboratory studies from boreal soils showing increased NO emissions with higher soil temperature (Koponen et al. 2006; Maljanen et al. 2007). This could primarily link with accelerated nitrification (AOB/AOA) and abiotic NO formation from NO_2^- at warmer soil temperatures (Butterbach-Bahl et al. 2013; Pilegaard 2013). This is also supported by significantly higher mean NNR indicating higher nitrification in vegetated surfaces compared to bare soil (Fig. 2c). Higher soil temperature increases microbial turnover and enzyme kinetics of soil nitrifiers (e.g., ammonia monooxygenase) and denitrifiers and can enhance chemo-denitrification of NO_2^-, elevating near-surface NO production and diffusional escape (Butterbach-Bahl et al. 2013; Pilegaard 2013) similar to HONO (Bhattarai et al. 2019, 2018; Maljanen et al. 2013; Oswald et al. 2013; Song et al. 2024; Su et al. 2011; Wu et al. 2019).

In contrast, N_2O emissions were exclusively temperature-driven (Fig. 5), with no significant direct or indirect effects of moisture, and vegetation induced shift to soil pH, and mineral N pools. These findings are consistent with earlier work in boreal ecosystems showing that N_2O emissions often increase with rising soil temperature (Buckeridge et al. 2020) although studies reporting no clear temperature dependence also exist (Maljanen et al. 2007), indicating that the strength of this relationship may vary across sites and conditions. Nevertheless, our N_2O results suggests that during early growth phase of vegetation in boreal soils, kinetic acceleration of nitrification and/or denitrification steps dominates N_2O production (Butterbach-Bahl et al. 2013), while moisture and substrate availability are not limiting. This interpretation is consistent with findings from our recent work, in which we identified a potential link between nitrification activity and N_2O emissions at the same site (Bhattarai et al. 2025). This sole and direct effect of temperature on N_2O emission is justified as we found no supported indirect pathways and no direct effects from mineral N or pH on N_2O.

Soil moisture reduces HONO and NO emissions whereas it exerts minimal effect on N_2O

Moisture exerted a negative effect (≈ –0.35, Fig. 5) on HONO fluxes indicating drier conditions favoured higher HONO release. Although soil moisture covaried with soil temperature, the SEM identified a direct negative moisture effect independent of the temperature pathway, consistent with surface dryness and diffusional access acting as key controls. This result agrees with previous studies showing lower HONO emissions at higher moisture (Cheng et al. 2025; Oswald et al. 2013; Song et al. 2023; Wu et al. 2019). We attribute this mainly to the diffusion barrier created by soil moisture. Under wet conditions, HONO emissions are reduced because more HONO dissolves in water, is re-adsorbed or consumed, and its movement through the soil slows down, making it harder for HONO to escape. Additionally, at higher soil moisture slow nitrification processes could be expected (Wu et al. 2019) which could further lower the HONO emissions. Some studies have reported HONO peaks at high soil moisture, driven either by microbial NO_3^- reduction to NO_2^- (Wu et al. 2019) or fertilizer-induced NO_2^- accumulation (Wang et al. 2021). In contrast, our results suggest a nitrification-dominated HONO and NO regime at our study site, although both nitrification and denitrification likely contributed to the overall HONO precursor, i.e., NO_2^- pool (Bhattarai et al. 2021). In addition to direct moisture effect, we also found that vegetation growth (plant height) indirectly suppressed HONO emissions (–0.19, Fig. 5) by increasing soil moisture. This points to a vegetation-mediated hydrological control during their early growth phase, likely driven by canopy shading, moderation of the soil-surface microclimate, reduced evaporative demand, and potential root-driven redistribution of water in the surface soil layers. In addition, young vegetation with relatively low evapotranspiration demand may have contributed to higher surface soil moisture retention, thereby slowing the HONO emission rates. Although NO_3^-, NO_2^-, and pH were interlinked, NO_3^- and pH jointly accelerates NO_2^- production, and NH_4^+ strongly favoured NO_3^- production, their direct effects on HONO were weak. This indicates that while mineral-N dynamics shape reactive N intermediates, they do not translate into HONO unless paired with conducive micro-environmental conditions. This agrees with the findings by Song et al. (2023), who highlighted soil water regimes and meteorology as key drivers of HONO emissions in managed fields.

A similar negative effect was also seen for NO emissions, however more strongly (≈ –0.60, Fig. 5) than HONO, emphasizing the dominant role of soil moisture in governing NO production and

consumption and its transport than HONO and agrees with previous research that have reported concurrent measurements of HONO and NO (Cheng et al. 2025). The influence of soil moisture on NO emissions is further corroborated by daily flux measurements during rainfall events, where both episodes exhibited a markedly stronger decline in NO emissions compared to HONO (Fig. 1a and Fig. 3). We infer this finding mainly with the effect of moisture on soil porosity as well as underlying oxic N-cycling process. It is well known that high soil moisture (e.g., water filled pore space, WFPS) reduces the extent of gas-filled porosity limiting the gaseous escape and inhibiting aerobic NO producing nitrification process (Pilegaard 2013). Further, high soil moisture can limit NO emission reducing it to N_2O or N_2 in denitrification (Davidson 1993; Pilegaard 2013). Our observation of NO-moisture relationship agrees with previous report from a boreal pasture soil that shows a higher NO emission with lower soil moisture (Maljanen et al. 2007) and a study by (Syväsalo et al. 2004) who highlights soil moisture (e.g., WFPS) as key predictor of reactive N-gas fluxes in boreal soils.

Based on SEM, soil moisture did not directly predict N_2O during early growth phase of vegetation at least for the duration of our study although it is well known that moisture promotes N_2O emissions via denitrification and nitrifier-denitrification, particularly where roots sustain carbon supply and create redox heterogeneity (Butterbach-Bahl et al. 2013). However, no considerable effect of moisture reflects few possibilities. A limited moisture range (average; $0.14-0.30$ g H_2O $g_{dw}{}^{-1}$; Fig. 2, corresponding to $26-56\%$ WFPS) during our study period, a short experimental duration, or micro-scale heterogeneity that kept denitrification substrates/electron acceptors below a threshold for a moisture effect to emerge. This is also further supported by a contrasting pattern of emission change during two precipitation events (Fig. 3) followed by varying strength of N_2O emissions between treatments (oat and barley vs. bare, Fig. 1a) after second precipitation, indicating in inconsistent moisture effect on N_2O emissions as vegetation grows. To reveal moisture or substrate controls, we suggest future studies to consider a longer time series with broader moisture variability (e.g., wetting/drying events) and functional gene profiling (*nirK*/*nirS*, *nosZ*) which could clarify whether electron acceptor limitation or N_2O reduction capacity (Hallin et al. 2018) modulates emissions under boreal conditions.

Early vegetation growth mediates soil chemistry more than direct impacts on gaseous emissions

At our study site, early vegetation growth phases appeared to drive rhizosphere processes, such as root exudate supply, proton release/uptake, and oxygen drawdown that shifted pH and NO_2^- availability more than they directly altered gas fluxes (Fig. 5). As plants developed, these changes likely modulated nitrification vs. denitrification kinetics and the aqueous–gas partitioning of HONO, yielding predictable shifts in the HONO and NO balance relative to N_2O for the period of our study. First, soil pH strongly influences NO_2^- speciation. At higher pH, NO_2^- is favoured over HONO, stabilizing NO_2^- in solution and increasing the potential substrate for HONO and NO when soils dry, whereas lower pH promotes protonation, leading to HONO and NO formation and loss (Donaldson et al. 2014; Su et al. 2011). Second, plant N uptake can drive rhizosphere alkalinization with NO_3^- uptake or acidification with NH_4^+ uptake, thereby steering both nitrifier communities (AOB/AOA) and NO_2^- stability (Pilegaard 2013; Prosser and Nicol 2008). Third, growth-related changes in root exudation and oxygen release reshape micro-redox mosaics, influencing the balance between nitrification, denitrification, and nitrifier-denitrification. Laboratory work shows that NO_2^- accumulation strongly stimulates HONO and NO_x (10–29% of added NO_2^- converted to HONO) and that the relative contribution of AOB/comammox versus AOA is pH- and soil-specific (Su et al. 2011; Bhattarai et al. 2021; Song et al. 2023).

Our findings indicate that N-gas emissions during early crop growth are more closely associated with vegetation-induced changes in soil chemistry than with direct vegetation involvement, at least over the study period. Increasing plant height was associated with reductions in pH and NO_2^- concentrations (Fig. 5), suggesting that shifts opposing acid–base equilibrium may limit HONO precursors and consequently suppress HONO emissions. The absence of significant direct effects of pH, NO_2^-, and NO_3^- on HONO implies that, under relatively stable redox and pH conditions typical of early growth stages, abiotic processes such as NO_2^- protonation and HONO volatilization are less influenced by N-pool concentrations than by soil moisture and temperature dynamics (Wu et al. 2019). This interpretation is supported by a marginally significant negative effect of vegetation

on HONO emissions. Additionally, the potential for HONO uptake by vegetative surfaces (e.g., leaves and branches) (Schimang et al. 2006; Sörgel et al. 2015) should be considered in future studies, as it may further contribute to observed emission patterns.

Our results for NO point to a transport-dominated regime rather than strong direct regulation by soil chemistry. The modest negative effect of plant height in the SEM is consistent with vegetation-mediated microclimatic and hydrologic influences, such as early canopy shading and altered evaporative demand that elevate near-surface moisture and thereby dampen NO fluxes (Malique et al. 2019; Pilegaard 2013). For N_2O, a similar interpretation is plausible if conditions favoured nitrifier pathways and/or complete denitrification to N_2 via *nosZ*-carrying organisms, limiting N_2O accumulation even as NO_2^- and NO_3^- varied (Butterbach-Bahl et al. 2013; Hallin et al. 2018; Venterea and Rolston 2000). The absence of a direct vegetation effect on N_2O despite vegetation influences on moisture and pH supports the view that microclimate (particularly temperature) was the immediate constraint on N_2O emissions during early crop stages, whereas soil–vegetation interactions primarily shaped NO_x/pH dynamics.

Interestingly, we observed significantly lower NO emissions ($p < 0.05$) in vegetated soils compared to bare soils (Fig. 1d), accompanied by a notably higher net nitrification rates (NNR; $p < 0.001$, Fig. 2c). This apparent mismatch suggests complex interactions between NO production and consumption pathways, influenced by soil moisture and plant-derived carbon. While a higher NNR implies active nitrification and potentially producing higher NO, yet denitrifiers in the same microsites may consume nitrifier-generated NO ($NO \rightarrow N_2O \rightarrow N_2$) (Medinets et al. 2015), reducing NO emissions to the atmosphere. Consequently, even with active nitrification, NO emissions may remain low due to intensified denitrification, especially during early vegetation growth, when soil microsites gradually shift between oxic and anoxic environment before strong effect of vegetation can emerge. Furthermore, vegetation can directly uptake NO_2 (and thus indirectly affect NO dynamics) via stomatal exchange (Chaparro-Suarez et al. 2011; Delaria et al. 2020). These mechanisms likely converge to produce both lower NO emissions and higher NNR under vegetation.

Collectively, the limited direct influence of individual soil variables underscores the need for integrated emission frameworks that consider all N-gases together and explicitly separate climate from substrate controls to clarify mechanistic pathways and improve process-based estimates. Future research should adopt this holistic approach while also examining both belowground and aboveground mechanisms, including plant-mediated N-gas uptake through stomata and microscale interactions between nitrifiers and denitrifiers in boreal agricultural soils.

Limitations of the study

While we provided first simultaneous *in-situ* emissions and causal insights into HONO, NO, and N_2O emissions during early growth phase of crops, our study has limitations. Our inference reflects an early growth window (0–15 days after sowing) at early period of growing season (early June) with a limited moisture range and potential microsite heterogeneity, which likely constrained the expression of substrate-driven controls. Focusing on the very early crop growth stage (0–15 days) restricts our ability to generalize findings across the full crop life cycle, during which plant development can markedly influence soil C and N dynamics and, consequently, gas fluxes. In addition, our study evaluates N-gas emissions primarily under growing-season conditions and does not account for boreal seasonal dynamics. Long non-growing periods, frost, and freeze–thaw cycles are known to strongly regulate N cycling and gaseous losses in these systems. Moreover, our study examined N-gas dynamics primarily as a function of vegetation-driven changes in soil properties, which limits understanding, especially of HONO because above-canopy and surface-atmosphere chemistry (e.g., $NO_2 \rightarrow$ HONO conversion) can also contribute considerably (Meng et al. 2024; Stemmler et al. 2006).

Directions for future research

Future research should extend measurements across the full crop life cycle to capture how emissions vary with plant development and associated shifts in soil C and N dynamics. Such studies will improve our understanding about whether root-exudate-driven microbial stimulation eventually exceeds plant–microbe competition for mineral N and leads to stronger vegetation effects on N-gas emissions. Year-round monitoring is also essential in boreal agroecosystems to quantify cumulative emissions and identify critical periods, especially during

freeze–thaw transitions and non-growing seasons, which remain poorly characterized for HONO and NO relative to N_2O (Koponen et al. 2006).

To strengthen mechanistic understanding, future studies should integrate gas flux measurements with microbial functional markers (e.g., *amoA*, *nirK/nirS*, *norB*, *nosZ*) and explicitly link emissions to nitrogen transformation pathways. Incorporating vegetation-mediated carbon inputs, particularly root exudates and labile carbon supply, together with pore-water NO_2^-/HNO_2 speciation, will be especially important for resolving HONO production mechanisms (Su et al. 2011; Song et al. 2023). Given the varying strengths of temperature and moisture sensitivities of HONO and NO versus N_2O, studies should also explore these relationships across varying N levels and soil types in boreal agroecosystem. Long-term, multi-season experiments that incorporate these factors will be essential for improving mechanistic understanding and enhancing predictive models of N-gas emissions and supporting sustainable agricultural practices under changing climate and management scenarios.

Conclusions

This study provides the first simultaneous *in-situ* evidence that boreal agricultural soils emit HONO, NO, and N_2O during the early crop growth phase. Emissions followed a consistent hierarchy, with N_2O dominating over NO and HONO, highlighting the importance of boreal agricultural soils as sources of both climate-relevant and atmospherically reactive N-gases. Across the measured gases, soil temperature emerged as the strongest positive driver, whereas soil moisture suppressed HONO and NO emissions however had limited direct influence on N_2O within the observed moisture range. Early vegetation growth influenced emissions mainly indirectly by modifying soil moisture, pH, and mineral N pools, rather than through strong direct effects on N-gas fluxes. These results show that, during early crop establishment, physical controls, particularly warming, drying, and gas transport constraints outweigh bulk chemical controls in regulating reactive N-gas emissions. These insights suggest that management practices aimed at buffering warm–dry soil conditions could help mitigate reactive N-gas losses from boreal agricultural soils. In particular, irrigation should be scheduled to avoid high-temperature and dry afternoon periods, when HONO and NO emissions are likely to peak, and should instead be timed to maintain moderate soil moisture during critical warm periods. Longer-term measurements across full crop phenology, combined with microbial functional gene analyses, are needed to determine when substrate-driven and microbial controls become dominant.

Authors contributions Hem Raj Bhattarai: Conceptualization (lead); writing-original draft (lead); data curation, formal analysis and visualization (lead); writing–reviewing and editing (equal). Maarit Liimatainen: Conceptualization, writing–reviewing and editing (equal). Narasinha J Shurpali: Funding acquisition for writing the article, writing–reviewing and editing (equal). Perttu Virkajärvi: writing–reviewing and editing (equal). Hannu Nykänen: writing–reviewing and editing (equal). Marja Maljanen: Conceptualization, funding acquisition (lead); writing–reviewing and editing (equal).

Funding Open access funding provided by Natural Resources Institute Finland. This study was funded by the Research Council of Finland under the projects *"The origin of nitrous acid (HONO) emissions from northern soils and linkages to nitrogen cycle processes"* (grant no. 297735) and *"Reactive N-Gas emissions across northern peatlands under changing climate conditions"* (grant no. 348571). We acknowledge considerable support by the Research Council of Finland through the project: *"Mechanism of nitrous oxide (N_2O) uptake in different cropping systems in different climate zones"*(ENSINK; grant no. 334422) and by the EU horizon research and innovation program through the projects: *"Sustainable soil and subsoil health promotion by implementing agroecological land use management to enhance ecosystem services"*(SUS-SOIL; GA ID: 101157560), *"Valorisation and eco-design of post-consumer wood waste into sustainable bio-based products"* (WoodVALOR; GA ID:101214964), and *"Climate Smart Research"* (CSR; GA ID: 101216573).

Data availability The data synthesized in this study will be made available in zenodo data repository.

Declarations

Conflict of interests All authors have no competing interests to disclose.

References

Atkinson R (2000) Atmospheric chemistry of VOCs and NO_x. Atmos Environ 34:2063–2101. https://doi.org/10.1016/S1352-2310(99)00460-4

Bates D, Mächler M, Bolker B, Walker S (2015) Fitting linear mixed-effects models using lme4. J Stat Soft 67. https://doi.org/10.18637/jss.v067.i01

Bhattarai HR, Virkajärvi P, Yli-Pirilä P, Maljanen M (2018) Emissions of atmospherically important nitrous acid (HONO) gas from northern grassland soil increases in the presence of nitrite (NO_2^-). Agric Ecosyst Environ 256:194–199. https://doi.org/10.1016/j.agee.2018.01.017

Bhattarai HR, Liimatainen M, Nykänen H, Kivimäenpää M, Martikainen PJ, Maljanen M (2019) Germinating wheat promotes the emission of atmospherically significant nitrous acid (HONO) gas from soils. Soil Biol Biochem 136:107518. https://doi.org/10.1016/j.soilbio.2019.06.014

Bhattarai HR, Wanek W, Siljanen HMP, Ronkainen JG, Liimatainen M, Hu Y, Nykänen H, Biasi C, Maljanen M (2021) Denitrification is the major nitrous acid production pathway in boreal agricultural soils. Commun Earth Environ 2:54. https://doi.org/10.1038/s43247-021-00125-7

Bhattarai HR, Marushchak ME, Ronkainen J, Lamprecht RE, Siljanen HMP, Martikainen PJ, Biasi C, Maljanen M (2022) Emissions of atmospherically reactive gases nitrous acid and nitric oxide from Arctic permafrost peatlands. Environ Res Lett 17:024034. https://doi.org/10.1088/1748-9326/ac4f8e

Bhattarai HR, Honkanen E, Ruhanen H, Soinnie H, Gil J, Saghir S, Lappalainen R, Shurpali NJ (2025) Effects of biochar, hydrochar and nitrogen fertilization on greenhouse gas fluxes, soil organic carbon pools, and biomass yield of a boreal legume grassland. Biochar 7:114. https://doi.org/10.1007/s42773-025-00496-6

Buckeridge KM, Edwards KA, Min K, Ziegler SE, Billings SA (2020) Short- and long-term temperature responses of soil denitrifier net N_2O efflux rates, inter-profile N_2O dynamics, and microbial genetic potentials. SOIL 6:399–412. https://doi.org/10.5194/soil-6-399-2020

Butterbach-Bahl K, Baggs EM, Dannenmann M, Kiese R, Zechmeister-Boltenstern S (2013) Nitrous oxide emissions from soils: how well do we understand the processes and their controls? Philos Trans R Soc B Biol Sci 368:20130122. https://doi.org/10.1098/rstb.2013.0122

Chaparro-Suarez IG, Meixner FX, Kesselmeier J (2011) Nitrogen dioxide (NO_2) uptake by vegetation controlled by atmospheric concentrations and plant stomatal aperture. Atmos Environ 45:5742–5750. https://doi.org/10.1016/j.atmosenv.2011.07.021

Cheng P, Han B, Tian Z, Liu Z, Yang W, Gu J, Yu X, Wang H, Zhou M (2025) Soil emissions of HONO and other nitrogen-containing gases: insights into microbial pathways and moisture effects. Atmos Pollut Res 16:102501. https://doi.org/10.1016/j.apr.2025.102501

Claeys M (2004) Formation of secondary organic aerosols through photooxidation of isoprene. Science 303:1173–1176. https://doi.org/10.1126/science.1092805

Coskun D, Britto DT, Shi W, Kronzucker HJ (2017) How plant root exudates shape the nitrogen cycle. Trends Plant Sci 22:661–673. https://doi.org/10.1016/j.tplants.2017.05.004

Davidson EA (1993) Soil water content and the ratio of nitrous oxide to nitric oxide emitted from soil. In: Oremland RS (ed) Biogeochemistry of global change. Springer US, Boston, MA, pp 369–386. https://doi.org/10.1007/978-1-4615-2812-8_20

Delaria ER, Place BK, Liu AX, Cohen RC (2020) Laboratory measurements of stomatal NO_2 deposition to native California trees and the role of forests in the NO_x cycle. Atmos Chem Phys 20:14023–14041. https://doi.org/10.5194/acp-20-14023-2020

Donaldson MA, Bish DL, Raff JD (2014) Soil surface acidity plays a determining role in the atmospheric-terrestrial exchange of nitrous acid. Proc Natl Acad Sci U S A 111:18472–18477. https://doi.org/10.1073/pnas.1418545112

Ermel M, Behrendt T, Oswald R, Derstroff B, Wu D, Hohlmann S, Stönner C, Pommerening-Röser A, Könneke M, Williams J, Meixner FX, Andreae MO, Trebs I, Sörgel M (2018) Hydroxylamine released by nitrifying microorganisms is a precursor for HONO emission from drying soils. Sci Rep 8. https://doi.org/10.1038/s41598-018-20170-1

FAO (2017) The future of food and agriculture: trends and challenges. Food and Agriculture Organization of the United Nations, Rome

Fawcett JK, Scott JE (1960) A rapid and precise method for the determination of urea. J Clin Pathol 13:156–159

Firestone M, Davidson E (1989) Microbiological basis of NO and N_2O production and consumption in soil. In: Andreae MO, Schimel DS (eds) Exchange of trace gases between terrestrial ecosystems and the atmosphere. Wiley, New York, pp 7–21

Firestone MK, Smith MS, Firestone RB, Tiedje JM (1979) The influence of nitrate, nitrite, and oxygen on the composition of the gaseous products of denitrification in soil. Soil Sci Soc Am J 43:1140–1144. https://doi.org/10.2136/sssaj1979.03615995004300060016x

Fox J, Weisberg S, Price B (2001) car: Companion to applied regression. https://doi.org/10.32614/CRAN.package.car

Galloway AF, Akhtar J, Burak E, Marcus SE, Field KJ, Dodd IC, Knox P (2022) Altered properties and structures of root exudate polysaccharides in a root hairless mutant of barley. Plant Physiol 190:1214–1227. https://doi.org/10.1093/plphys/kiac341

Gao X, Deng O, Ling J, Zeng M, Lan T (2018) Effects of controlled-release fertilizer on nitrous oxide and nitric oxide emissions during wheat-growing season: field and pot experiments. Paddy Water Environ 16:99–108. https://doi.org/10.1007/s10333-017-0619-6

Hallin S, Philippot L, Löffler FE, Sanford RA, Jones CM (2018) Genomics and ecology of novel N_2O-reducing microorganisms. Trends Microbiol 26:43–55. https://doi.org/10.1016/j.tim.2017.07.003

Hartig F (2016) DHARMa: Residual diagnostics for hierarchical (Multi-Level / Mixed) regression models. https://doi.org/10.32614/CRAN.package.DHARMa

Heland J, Kleefmann J, Kurtenbach R, Wiesen P (2001) A new instrument to measure gaseous nitrous acid (HONO) in the atmosphere. Environ Sci Technol 35:3207–3212

Hinsinger P, Bengough AG, Vetterlein D, Young IM (2009) Rhizosphere: biophysics, biogeochemistry and ecological relevance. Plant Soil 321:117–152. https://doi.org/10.1007/s11104-008-9885-9

Jones DL, Hodge A, Kuzyakov Y (2004) Plant and mycorrhizal regulation of rhizodeposition. New Phytol 163:459–480. https://doi.org/10.1111/j.1469-8137.2004.01130.x

Kleffmann J, Heland J, Kurtenbach R, Lörzer J, Wiesen P (2002) A new instrument (LOPAP) for the detection of nitrous Acid (HONO). Environ Sci Pollut Res 48–54

Koponen HT, Escudé Duran C, Maljanen M, Hytönen J, Martikainen PJ (2006) Temperature responses of NO and N_2O emissions from boreal organic soil. Soil Biol Biochem 38:1779–1787. https://doi.org/10.1016/j.soilbio.2005.12.004

Kulmala M, Petaja T (2011) Soil nitrites influence atmospheric chemistry. Science 333:1586–1587. https://doi.org/10.1126/science.1211872

Kuzyakov Y (2002) Review: factors affecting rhizosphere priming effects. J Plant Nutr Soil Sci 165:382–396. https://doi.org/10.1002/1522-2624(200208)165:4/3C382::AID-JPLN382/3E3.0.CO;2-23

Kuzyakov Y (2010) Priming effects: interactions between living and dead organic matter. Soil Biol Biochem 42:1363–1371. https://doi.org/10.1016/j.soilbio.2010.04.003

Kuzyakov Y, Xu X (2013) Competition between roots and microorganisms for nitrogen: mechanisms and ecological relevance. New Phytol 198:656–669. https://doi.org/10.1111/nph.12235

Lefcheck JS (2016) PiecewiseSEM: piecewise structural equation modelling in r for ecology, evolution, and systematics. Methods Ecol Evol 7:573–579. https://doi.org/10.1111/2041-210X.12512

Lelieveld J, Dentener FJ, Peters W, Krol MC (2004) On the role of hydroxyl radicals in the self-cleansing capacity of the troposphere. Atmos Chem Phys 4:2337–2344. https://doi.org/10.5194/acp-4-2337-2004

Lelieveld J, Gromov S, Pozzer A, Taraborrelli D (2016) Global tropospheric hydroxyl distribution, budget and reactivity. Atmos Chem Phys 16:12477–12493. https://doi.org/10.5194/acp-16-12477-2016

Lind SE, Shurpali NJ, Peltola O, Mammarella I, Hyvönen N, Maljanen M, Räty M, Virkajärvi P, Martikainen PJ (2016) Carbon dioxide exchange of a perennial bioenergy crop cultivation on a mineral soil. Biogeosciences 13:1255–1268. https://doi.org/10.5194/bg-13-1255-2016

Linn DM, Doran JW (1984) Effect of water-filled pore space on carbon dioxide and nitrous oxide production in tilled and nontilled soils. Soil Sci Soc Am J 48:1267–1272. https://doi.org/10.2136/sssaj1984.03615995004800060013x

Lu P, Yang T, Li L, Zhao B, Liu J (2020) Response of oat morphologies, root exudates, and rhizosphere fungal communities to amendments in a saline-alkaline environment. PLoS ONE 15:e0243301. https://doi.org/10.1371/journal.pone.0243301

Malique F, Ke P, Boettcher J, Dannenmann M, Butterbach-Bahl K (2019) Plant and soil effects on denitrification potential in agricultural soils. Plant Soil 439:459–474. https://doi.org/10.1007/s11104-019-04038-5

Maljanen M, Martikkala M, Koponen H, Virkajarvi P, Martikainen P (2007) Fluxes of nitrous oxide and nitric oxide from experimental excreta patches in boreal agricultural soil. Soil Biol Biochem 39:914–920. https://doi.org/10.1016/j.soilbio.2006.11.001

Maljanen M, Yli-Pirilä P, Hytönen J, Joutsensaari J, Martikainen PJ (2013) Acidic northern soils as sources of atmospheric nitrous acid (HONO). Soil Biol Biochem 67:94–97. https://doi.org/10.1016/j.soilbio.2013.08.013

Maljanen M, Gondal Z, Bhattarai HR (2016) Emissions of nitrous acid (HONO), nitric oxide (NO), and nitrous oxide (N_2O) from horse dung. Agric Food Sci 25:225–229

Maljanen M, Bhattarai HR, Biasi C, Sigurdsson BD (2018) The effect of geothermal soil warming on the production of carbon dioxide (CO_2), methane (CH_4), nitrous oxide (N_2O), nitric oxide (NO) and nitrous acid (HONO) from forest soil in southern Iceland. Icel Agric Sci 31:11–22. https://doi.org/10.16886/IAS.2018.02

Maljanen ME, Marttila E, Bhattarai HR (2023) Greenhouse gas and reactive N-gas emissions from a horse paddock – relationship to physicochemical properties of soil. Afsci. https://doi.org/10.23986/afsci.130086

Medinets S, Skiba U, Rennenberg H, Butterbach-Bahl K (2015) A review of soil NO transformation: associated processes and possible physiological significance on organisms. Soil Biol Biochem 80:92–117. https://doi.org/10.1016/j.soilbio.2014.09.025

Meng F, Han B, Qin M, Fang W, Tang K, Shao D, Liao Z, Duan J, Feng Y, Huang Y, Ni T, Xie P (2024) Measurement report: surface exchange fluxes of HONO during the growth process of paddy fields in the Huaihe River Basin, China. Atmos Chem Phys 24:14191–14208. https://doi.org/10.5194/acp-24-14191-2024

Ndah FA, Maljanen M, Rinnan R, Bhattarai HR, Davie-Martin CL, Mikkonen S, Michelsen A, Kivimäenpää M (2024) Carbon and nitrogen-based gas fluxes in subarctic ecosystems under climate warming and increased cloudiness. Environ Sci Atmos 4:942–957. https://doi.org/10.1039/D4EA00017J

Nguyen C (2003) Rhizodeposition of organic C by plants: mechanisms and controls. Agronomie 23:375–396. https://doi.org/10.1051/agro:2003011

Oswald R, Behrendt T, Ermel M, Wu D, Su H, Cheng Y, Breuninger C, Moravek A, Mougin E, Delon C, Loubet B, Pommerening-Roser A, Sorgel M, Poschl U, Hoffmann T, Andreae MO, Meixner FX, Trebs I (2013) HONO emissions from soil bacteria as a major source of atmospheric reactive nitrogen. Science 341:1233–1235. https://doi.org/10.1126/science.1242266

Pilegaard K (2013) Processes regulating nitric oxide emissions from soils. Philos Trans R Soc B Biol Sci 368:20130126. https://doi.org/10.1098/rstb.2013.0126

Pirinen P (2012) Tilastpja suomen ilmastosta 1981-2010. Ilmatieteen Laitos, Helsinki

Prosser JI, Nicol GW (2008) Relative contributions of archaea and bacteria to aerobic ammonia oxidation in the environment. Environ Microbiol 10:2931–2941. https://doi.org/10.1111/j.1462-2920.2008.01775.x

Ravishankara AR, Daniel JS, Portmann RW (2009) Nitrous oxide (N_2O): the dominant ozone-depleting substance emitted in the 21st century. Science 326:123–125. https://doi.org/10.1126/science.1176985

Regina K, Nykänen H, Maljanen M, Silvola J, Martikainen PJ (1998a) Emissions of N_2 O and NO and net nitrogen mineralization in a boreal forested peatland treated with different nitrogen compounds. Can J for Res 28:132–140. https://doi.org/10.1139/x97-198

Regina K, Silvola J, Martikainen PJ (1998b) Mechanisms of N_2O and NO production in the soil profile of a drained and forested peatland, as studied with acetylene, nitrapyrin and dimethyl ether. Biol Fertil Soils 27:205–210. https://doi.org/10.1007/s003740050421

Robertson GP, Groffman PM (2015) Nitrogen transformations. In: Paul EA (ed) Soil microbiology, ecology and biochemistry, 4th edn. Academic Press, Burlington MA, pp 421–446

Robertson GP, Coleman DC, Bledsoe CS, Sollins P (1999) Standard soil methods for long-term ecological research. Oxford University Press, New York

Scharko NK, Schütte UME, Berke AE, Banina L, Peel HR, Donaldson MA, Hemmerich C, White JR, Raff JD (2015) Combined flux chamber and genomics approach links nitrous acid emissions to ammonia oxidizing bacteria and archaea in urban and agricultural soil. Environ Sci Technol 49:13825–13834. https://doi.org/10.1021/acs.est.5b00838

Schimang R, Folkers A, Kleffmann J, Kleist E, Miebach M, Wildt J (2006) Uptake of gaseous nitrous acid (HONO) by several plant species. Atmos Environ 40:1324–1335. https://doi.org/10.1016/j.atmosenv.2005.10.028

Searle SR, Speed FM, Milliken GA (1980) Population marginal means in the linear model: an alternative to least squares means. Am Stat 34:216–221. https://doi.org/10.1080/00031305.1980.10483031

Shipley B (2000) A new inferential test for path models based on directed acyclic graphs. Struct Equ Model 7:206–218. https://doi.org/10.1207/S15328007SEM0702_4

Singmann H, Bolker B, Westfall J, Aust F, Ben-Shachar MS (2012) afex: analysis of factorial experiments. https://doi.org/10.32614/CRAN.package.afex

Song Y, Wu D, Ju X, Dörsch P, Wang M, Wang R, Song X, Deng L, Wang R, Gao Z, Haider H, Hou L, Liu M, Yu Y (2023) Nitrite stimulates HONO and NO_x but not N_2O emissions in Chinese agricultural soils during nitrification. Sci Total Environ 902:166451. https://doi.org/10.1016/j.scitotenv.2023.166451

Song Y, Zhang Y, Tan M, Hu Y, Liu P, Tian D, Mu Y (2024) Annual emissions of N_2O, NO, HONO, and NH_3 from maize-wheat fields in the North China Plain. Sci Total Environ 954:176602. https://doi.org/10.1016/j.scitotenv.2024.176602

Sörgel M, Trebs I, Wu D, Held A (2015) A comparison of measured HONO uptake and release with calculated source strengths in a heterogeneous forest environment. Atmos Chem Phys Discuss 15:2119–2155. https://doi.org/10.5194/acpd-15-2119-2015

Stemmler K, Ammann M, Donders C, Kleffmann J, George C (2006) Photosensitized reduction of nitrogen dioxide on humic acid as a source of nitrous acid. Nature 440:195–198. https://doi.org/10.1038/nature04603

Su H, Cheng Y, Oswald R, Behrendt T, Trebs I, Meixner FX, Andreae MO, Cheng P, Zhang Y, Poschl U (2011) Soil nitrite as a source of atmospheric HONO and OH radicals. Science 333:1616–1618. https://doi.org/10.1126/science.1207687

Syväsalo E, Regina K, Pihlatie M, Esala M (2004) Emissions of nitrous oxide from boreal agricultural clay and loamy sand soils. Nutr Cycl Agroecosyst 69:155–165. https://doi.org/10.1023/B:FRES.0000029675.24465.fc

Tang K, Qin M, Fang W, Duan J, Meng F, Ye K, Zhang H, Xie P, Liu J, Liu W, Feng Y, Huang Y, Ni T (2020) An automated dynamic chamber system for exchange flux measurement of reactive nitrogen oxides (HONO and NO_X) in farmland ecosystems of the Huaihe River Basin, China. Sci Total Environ 745:140867. https://doi.org/10.1016/j.scitotenv.2020.140867

Tian H et al (2020) A comprehensive quantification of global nitrous oxide sources and sinks. Nature 586:248–256. https://doi.org/10.1038/s41586-020-2780-0

Venterea RT, Rolston DE (2000) Mechanisms and kinetics of nitric and nitrous oxide production during nitrification in agricultural soil. Glob Change Biol 6:303–316. https://doi.org/10.1046/j.1365-2486.2000.00309.x

Wang Y, Fu X, Wu D, Wang M, Lu K, Mu Y, Liu Z, Zhang Y, Wang T (2021) Agricultural fertilization aggravates air pollution by stimulating soil nitrous acid emissions at high soil moisture. Environ Sci Technol 55:14556–14566. https://doi.org/10.1021/acs.est.1c04134

Wang Y, Li Q, Wang Y, Ren C, Saiz-Lopez A, Xue L, Wang T (2025) Increasing soil nitrous acid emissions driven by climate and fertilization change aggravate global ozone pollution. Nat Commun 16:2463. https://doi.org/10.1038/s41467-025-57161-6

Wei T, Simko V (2010) corrplot: Visualization of a correlation matrix. https://doi.org/10.32614/CRAN.package.corrplot

Wu D, Horn MA, Behrendt T, Müller S, Li J, Cole JA, Xie B, Ju X, Li G, Ermel M, Oswald R, Fröhlich-Nowoisky J, Hoor P, Hu C, Liu M, Andreae MO, Pöschl U, Cheng Y, Su H, Trebs I, Weber B, Sörgel M (2019) Soil HONO emissions at high moisture content are driven by microbial nitrate reduction to nitrite: tackling the HONO puzzle. ISME J. https://doi.org/10.1038/s41396-019-0379-y

Zhu G et al (2025) Nitrous oxide sources, mechanisms and mitigation. Nat Rev Earth Environ 6:574–592. https://doi.org/10.1038/s43017-025-00707-5